free from blood, the perfusate was changed to a mixture of 3 percent glutaraldehyde, 3 percent paraformaldehyde, and 0.1 percent picric acid in 0.1*M* cacodylate buffer at *p*H 7.4. After perfusion, the spinal cord was sectioned (500 μm), and the appropriate slices were fixed in 1 percent osmium tetroxide and 1.5 percent potassium ferricyanide in 0.1*M* cacodylate buffer at *p*H 7.4 (*3*). The slices were then stained with 1 percent aqueous uranyl acetate, dehydrated, and embedded in a mixture of Epon and Araldite. Thin sections of the posterior columns were placed on single-hole grids covered by a Formvar film, and all myelinated and unmyelinated axons were counted.

The dorsal white funiculi in the rat are two large bundles of white matter that lie between the dorsal horns. At the light microscopic level, the most prominent components of these tracts are the myelinated axons, but capillaries and radial glial processes are also evident. The corticospinal tracts, which are located in the dorsal white column in the rat (*4*), are clearly indicated as small areas of closely spaced, fine, myelinated axons.

In the electron microscope, the above features are seen with greater clarity. In addition, the unmyelinated fibers can be seen (Fig. 1). In cross section, these axons have circular or oval profiles with diameters of 0.3 to 1.0 μm (Fig. 1). The organelles in these axons consist of neurofilaments, microtubules, and occasional mitochrondia (Fig. 1). The unmyelinated axons occur singly or in bundles of two to ten, and they are scattered throughout the funiculus and are not concentrated next to the gray matter or in the corticospinal tract. There are more unmyelinated than myelinated axons, both in the corticospinal tract and in the rest of the funiculus (Table 1). From these data, it can be calculated that 60 percent of the axons in the posterior funiculus of the rat are unmyelinated.

The fiber types that are known are (i) ascending myelinated primary afferent axons that are generally believed to be the predominant axonal type in the pathway, (ii) descending myelinated primary afferent axons located in the fasciculus interfascicularis (comma tract of Schultze) and septomarginal band (*5*), (iii) corticospinal fibers, which form a circumscribed bundle of axons in the ventromedial part of each posterior funiculus in the rat (*4*), (iv) propriospinal fibers (*5*), (v) fibers descending from cells in the nuclei gracilis and cuneatus (*6*), and (vi) second-order ascending cells (*7*).

It is possible that the unmyelinated axons also belong to one of these categories. Unmyelinated fibers outside of the corticospinal tract were mentioned by Nageotte (*8*), who noted a few unmyelinated fibers near the gray matter and in the median septum. The fact that the unmyelinated axons are spread throughout the funiculus suggests that they are not restricted to corticospinal or propriospinal systems, and it would be interesting to find unmyelinated primary afferent fibers in the posterior funiculi. The cell bodies that give rise to the unmyelinated axons can be located by various types of experimental surgery. Presumably an understanding of the unmyelinated fiber systems of the posterior funiculus will provide further insights into the organization of somatic sensory systems.

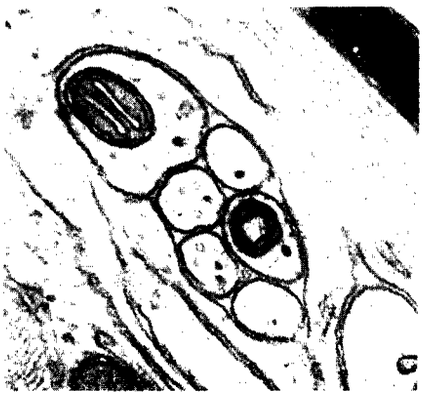

Fig. 1. A group of six unmyelinated fibers in the dorsal white colume (×90,000).

LAUREN A. LANGFORD
RICHARD E. COGGESHALL
Marine Biomedical Institute, University of Texas Medical Branch, Galveston 77550

References and Notes

1. S. W. Ranson and S. L. Clark, *The Anatomy of the Nervous System, Its Development and Function* (Saunders, Philadelphia, 1953), pp. 167–184; E. C. Crosby, T. Humphrey, E. W. Lauer, *Correlative Anatomy of the Nervous System* (Macmillan, New York, 1962), pp. 56–111; M. B. Carpenter, *Human Neuroanatomy* (Williams & Wilkins, Baltimore, 1976), pp. 238–284.
2. Y. C. Hwang, E. J. Hinsman, O. F. Roesel, *J. Comp. Neurol.* **162**, 195 (1962); A. Onishi, P. C. O'Brien, H. Okayoki, P. J. Dyck, *J. Neurol. Sci.* **77**, 163 (1976).
3. L. A. Langford and R. E. Coggeshall, *Anat. Rec.* **197**, 297 (1980).
4. S. W. Ranson, *Am. J. Anat.* **14**, 411 (1913); A. J. Linowiecki, *J. Comp. Neurol.* **24**, 509 (1914); P. W. Nathan and M. C. Smith, *Brain* **82**, 610 (1959); F. Valverde, *Z. Zellforsch. Mikrosk, Anat.* **71**, 297 (1966).
5. P. W. Nathan and M. C. Smith, *Brain* **82**, 610 (1959).
6. A. M. Dart, *J. Physiol (London)* **219**, 29 (1971); H. G. J. M. Kuypers and V. A. Maisky, *Neurosci. Lett.* **1**, 9 (1975); H. Burton and A. D. Loewy, *Brain Res.* **116**, 485 (1976).
7. N. Uddenberg, *Exp. Brain Res.* **4**, 377 (1968); A. Rustoni, *Brain Res.* **51**, 81 (1973); *ibid.* **75**, 247 (1974); D. Angaut-Petit, *Exp. Brain Res.* **22**, 457 (1975).
8. J. Nageotte, *Nouv. Iconog. Salpêt.* **17**, 2 (1904).
9. This work was supported by grants NS 10161, NS 07377, and NS 11255 from the National Institutes of Health.

25 July 1980; revised 22 September 1980

Assessment of Pharmacological Treatment of Myocardial Infarction by Phosphorus-31 NMR with Surface Coils

Abstract. *Phosphorus-31 nuclear magnetic resonance (NMR) measurements with small surface coils have been used to observe phosphorus metabolism of perfused hearts within localized regions. The method allows for direct, noninvasive, sequential assessment of the altered regional metabolism resulting from myocardial infarction and its response to drug treatment, which cannot be observed by conventional techniques.*

A central issue in the study of most disease states is the correlation between the pathophysiology and the metabolic competence of the region that incurs injury or exhibits an abnormality. This problem is of particular importance for conditions that involve compromised blood flow to and oxygenation of an organ or part of an organ. Myocardial infarction and cerebrovascular occlusion (stroke) are two examples. Key elements in the clinical treatment of infarction and stroke are the determination of the location, size, and extent of the injury and learning the time course of metabolic impairment and the onset of irreversible damage. Techniques based on x-rays, ultrasound, and nuclear medicine may be used to determine the size and location of injury, but there has been no clinical method for directly and noninvasively assessing the metabolic competence of an injured site. A method for noninvasively determining metabolic function would be extremely useful for characterizing the extent of deterioration and monitoring the efficacy of therapies.

Nuclear magnetic resonance (NMR) techniques can provide information on the molecular level about structural, motional, and thermodynamic properties of many naturally occurring nuclei of biological interest (*1*). The ^{31}P nucleus is useful in metabolic studies involving

0036-8075/81/0109-0177$00.50/0

compounds such as adenosine triphosphate (ATP), phosphocreatine (PCr), adenosine diphosphate (ADP), and inorganic phosphate (Pi). Phosphorus-31 NMR has been used to study cellular metabolism (*2*) and the metabolism of nearly all perfusible organs in vivo (*3*). Metabolism has also been studied by NMR with the ^{13}C, ^{1}H, and ^{2}H nuclei (*4*).

In this report we use the term ischemia to denote a condition of perfusion insufficient to provide adequate oxygen and substrate levels to the heart tissue. Regional heart ischemia was first investigated by noninvasive ^{31}P NMR by Hollis *et al.* (*5*), who used a conventional NMR receiver coil configuration that afforded no spatial selectivity. They observed a small signal attributable to Pi at an acidic *p*H when a regional infarction was produced by ligation of a major coronary artery. Changes in levels of other phosphate metabolites within the ischemic zone could not be detected (compare the spectra in Fig. 1, a and b), nor could the location of the ischemic region be determined. Ackerman *et al.* (*6*) used flat surface coils to map the distribution of phosphorylated metabolites in the brains and limbs of whole animals by ^{31}P NMR. Their work suggested that the surface coil method could be used to study regional ischemia in heart and brain.

We report here the application of small, flat surface coils to measure regional metabolism in perfused hearts by ^{31}P NMR. We have used this method to study the effects of localized infarction on phosphorus metabolism and the efficacy of treatment with the drugs verapamil and chlorpromazine. Verapamil is used in the clinical management of cardiac arrhythmias and angina. It is a potent negative inotropic substance that selectively reduces membrane transport of calcium ions. This activity appears to account for its coronary vasodilator properties and its ability to decrease oxygen consumption in myocardium (*7*). It has also been reported that verapamil maintains the functional and structural properties of heart mitochondria under conditions of oxygen deprivation (*8*). Chlorpromazine prevents irreversible mitochondrial damage in hepatic cells subjected to long periods of ischemia (*9*), apparently by preventing phospholipid breakdown during periods of anoxia. It also inhibits cellular calcium ion transport. To determine the ability of these drugs to inhibit the deleterious effects of regional infarction in perfused rabbit hearts, we treated them before ligation of the coronary artery. Verapamil was also used after ischemia was produced to assess its ability to reverse the metabolic degradation produced by the regional infarct. Sequential spectra were obtained to determine the time course of metabolic changes associated with the pharmacologic treatment.

Hearts were obtained from anesthetized New Zealand White rabbits (body weight, 1.0 to 1.5 kg) and perfused at 37°C by the Langendorff technique (*5*). Regional ischemia was produced by ligation of the left anterior descending coronary artery (LAD) above the septal branch (Fig. 1). The area of ischemia covered about 30 to 40 percent of the left ventricular anterior wall, as estimated by staining with methylene blue dye injected as a single bolus (50 ml, 0.05 percent) at the end of experiments that involved no drug treatment. The dye method was also used to confirm the placement of the surface coil in relation to the ischemic re-

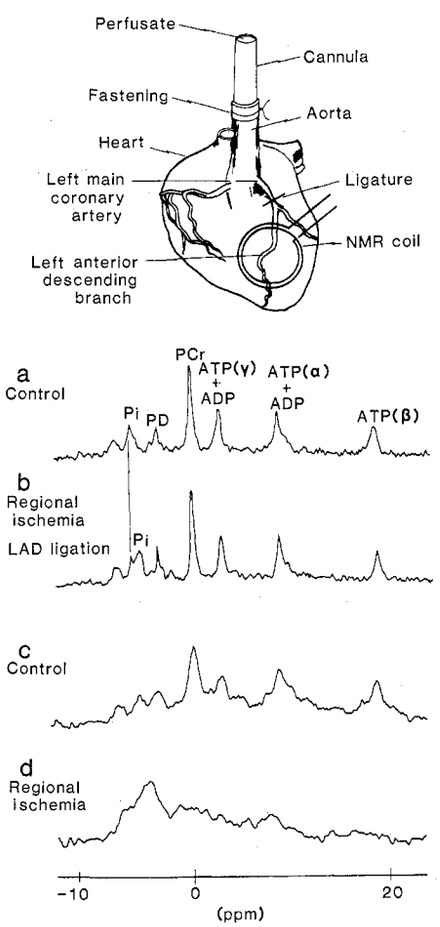

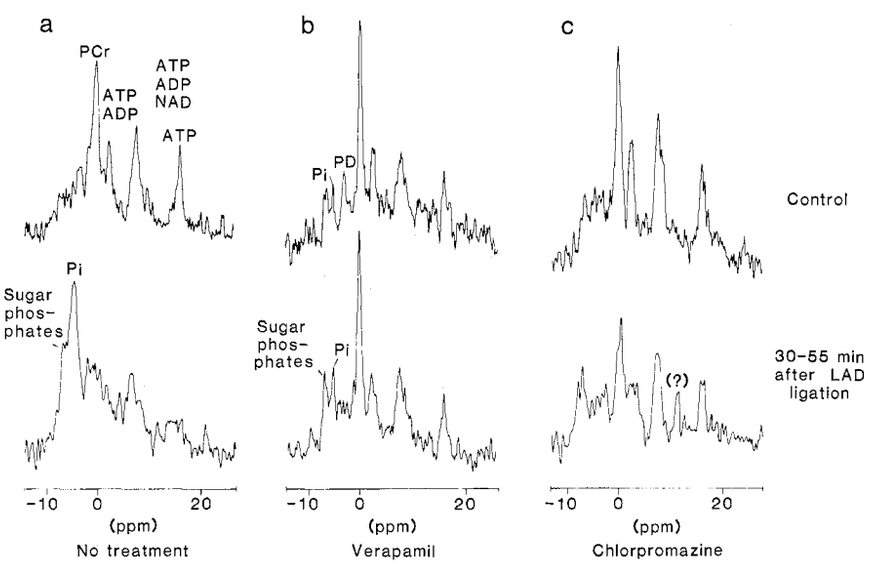

Fig. 1 (left). (Top) Diagram of a perfused heart showing the location of the ligature used in producing a localized ischemic area in the left ventricle. For surface coil experiments a small coil was positioned approximately as depicted. (a) A 5-minute spectrum (150 transients) from an entire, well-perfused heart. The spectrum was obtained with a conventional NMR probe. (b) Spectrum obtained as in (a) after ligation of the LAD. (c) Spectrum of the left ventricular area of a well-perfused heart obtained in 25 minutes (1000 transients) with a surface coil of 8-mm inner diameter [compare with (a)]. (d) Spectrum obtained as in (c) but for the 25-minute period immediately after LAD ligation with the surface coil placed on the surface of the heart below the ligature [compare with (b)]. Chemical shifts are indicated relative to the PCr resonance. In (a) and (c) the intracellular *p*H is ~ 7.1; in (b) the apparent *p*H of the ischemic region is ~ 6.4 and in (d) ~ 6.15. These *p*H values were determined from the chemical shifts of the Pi peaks relative to the PCr peak. Peak assignments: *Pi*, inorganic phosphate; *PD*, phosphodiester(?); *PCr*, phosphocreatine; *ATP*, adenosine triphosphate; and *ADP*, adenosine diphosphate. Fig. 2 (right). (a) Spectra for a normally oxygenated and regionally ischemic area of the left ventricle of a perfused heart. (b) Same sequence for a heart treated with verapamil and then subjected to LAD ligation. (c) Comparative sequence for chlorpromazine treatment. All spectra were obtained with a surface coil. Control spectra (at the top in each panel) were obtained before LAD ligation; spectra from the ischemic region (below) were obtained for the time interval indicated. The surface coil was placed in approximately the same location for control spectra and spectra from the ischemic region.

gion. The LAD serves as a marker for placement of the flat coil in the same location when observing normoxic and ischemic conditions.

Two protocols for drug administration were followed. In protocol 1, chlorpromazine (30 mg/kg) in normal saline was administered by intraperitoneal injection 50 minutes before excision and perfusion of the heart. Verapamil (1 mg/liter) was added directly to the perfusate at least 5 minutes before LAD ligation. In protocol 2, verapamil (1 mg/liter) was added to the perfusate at a fixed interval after LAD ligation.

The ^{31}P NMR spectra were obtained at 72.88 MHz, using a Bruker WH-180 NMR spectrometer and a superconducting magnet with a 90-mm bore. The spectra resulted from signal-averaging 1000 free induction decays and Fourier-transforming the resultant signal. The data acquisition period was 25 minutes per spectrum. Flat surface coils with either three turns and an inner diameter of 8 mm or two turns and an inner diameter of 11 mm were used for all measurements. The spatial selectivity of these coils is approximately confined to a volume subtended by the coil circumference and one radius deep from the coil center (*6*). A special NMR probe insert permitting broadband proton decoupling was used. The decoupler coils were also employed for adjusting the homogeneity of the main applied magnetic field by using the proton NMR signal of each heart. By appropriate translation and reorientation of the heart, the surface coil can be positioned anywhere on its exterior surface. Details of the insert, the measured nuclear Overhauser enhancement resulting from the broadband proton decoupling, and the mixing unit for the lock channel will be published (*10*).

The ^{31}P NMR spectra in Fig. 1, a and b, were obtained from normoxic and regionally ischemic hearts in a conventional NMR probe configuration with no spatial selectivity. The spectra in Fig. 1, c and d, were obtained with a surface coil located at a site on the left ventricle for control and ischemic conditions, respectively. The advantage of using the surface coils is evident. The spectrum in Fig. 1d shows significant alterations of the PCr and adenine nucleotide concentrations in the affected region, as well as a very broad phosphate signal centered about the PCr, Pi, and sugar phosphate resonances. These are imperceptible in the corresponding conventional spectrum in Fig. 1b.

The effects of verapamil and chlorpromazine pretreatment (protocol 1) are shown in Fig. 2. Hearts pretreated with verapamil retained nearly normal levels of phosphorylated metabolites (PCr and ATP) in the region of the left ventricle made ischemic by LAD ligation (Fig. 2, a and b). Chlorpromazine had a less dramatic but observable effect (Fig. 2c).

Figure 3 shows the time course of development of altered metabolism during ischemia and the reversal of these effects by subsequent administration of verapamil (protocol 2). The increase in concentration of PCr after administration of the drug may be seen by comparing the spectra in Fig. 3, c and e. The average of three separate determinations showed a 220 percent increase in PCr level after verapamil administration.

Several points about the experimental techniques and results should be discussed. The line widths vary greatly

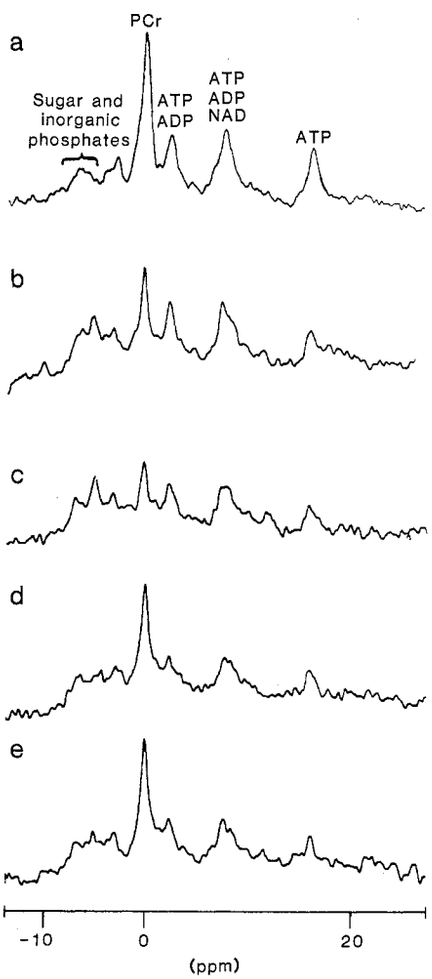

Fig. 3. Chronological sequence of spectra obtained with a surface coil before and after verapamil treatment in the regionally ischemic zone of a single heart. (a) Control spectrum, (b) spectrum obtained between 5 and 30 minutes after LAD ligation, (c) spectrum obtained between 30 and 55 minutes after ligation, (d) in the 5- to 30-minute interval after administration of verapamil (60 to 85 minutes postligation), and (e) 30 to 55 minutes after the start of verapamil treatment (85 to 110 minutes after ligation).

from one heart specimen to the next. This may be the result of several factors. First, the hearts were beating vigorously within the insert of the probe and the surface coil was not normally secured to the heart. The motion of the heart relative to the stationary surface coil is expected to produce some line broadening. We were able to obtain somewhat narrower lines by securing the coil to the surface of the heart with sutures or by packing cotton cloth around the exterior of the heart to reduce its freedom of movement. Second, the filling and emptying of the heart during the cardiac cycle may produce some line broadening. Verapamil-treated hearts generally gave narrower spectral lines, probably as a result of diminution of the force (and thus motion) of contraction.

The ^{31}P NMR results are consistent with the hypothesis that verapamil produces coronary vasodilation and therefore is likely to enhance collateral flow to the ischemic region (methylene blue dye injection supports this). The results obtained when the perfused hearts were treated with verapamil before LAD ligation indicate that this compound may also protect mitochondria under conditions of anoxia; however, we cannot rule out the possibility that the observed effect is solely the result of enhanced collateral flow.

Chlorpromazine has no apparent vascular effects but does provide sustained phosphorylated substrate levels in the absence of oxygenation. As noted earlier, chlorpromazine apparently prevents phospholipid depletion in mitochondria associated with ischemia or hypoxia (*9*). This may result in retention of an effective permeability barrier to calcium ions, preventing influx of calcium and formation of calcium phosphate precipitates within mitochondria. Spectra from chlorpromazine-treated hearts show a resonance slightly upfield of the α-resonance of ATP (Fig. 2c). This resonance is as yet unassigned, but has been observed in several spectra obtained from normoxic and ischemic hearts at markedly lower concentrations.

We consistently saw a diffuse, broad resonance most prominent in the sugar phosphate and Pi region of the spectra obtained from areas of ischemia in untreated LAD-ligated hearts (Fig. 1d). This may be a ^{31}P NMR signal from calcium phosphate precipitates in cells with damaged mitochondria (*11*). Preliminary ^{31}P NMR experiments on calcium phosphate precipitates support this tentative assignment. Phosphate metabolite levels are preserved in KCl-arrested hearts made globally ischemic (*12*) and a similar

result is found for regional ischemia by ^{31}P NMR surface coil measurements (*10*). The implication is that reducing work load and contractility helps to preserve ischemic myocardium.

Several possible extensions of the experiments reported here are foreseeable. Two or more surface coils could be used simultaneously to obtain spectra from different regions of the heart. A small coil could be placed inside the left ventricle of the perfused heart through a small incision in the left atrium to monitor the ^{31}P NMR spectrum from the interior myocardium. With a conventional transmitter coil and a small surface coil in a cross-coil configuration (*13*), one could measure other parameters such as relaxation times, diffusion coefficients, and the flow at well-defined locations in the heart and other organs. By use of surface coils, enzyme kinetic rates could be observed by saturation transfer techniques (*14*) for specific regions within the heart as a function of normal, pathological, and drug-treated states. Changes in phosphate substrate levels within localized volumes could be directly observed and related to the function of particular regions (for example, left ventricle versus left atrium) and to the contraction-relaxation cycle of the heart.

Our results, together with recent work by Grove *et al.* (*15*) on the determination of whole heart metabolism by ^{31}P NMR in vivo, indicate that surface coil NMR may eventually be used in vivo to assess the location and size of an injury or abnormality and determine the efficacy of drug treatment.

RAY L. NUNNALLY
Department of Radiology, University of Texas Health Science Center, Dallas 75235
PAUL A. BOTTOMLEY
General Electric Company Research and Development Center, Schenectady, New York 12301

References and Notes

1. R. A. Dwek, *Nuclear Magnetic Resonance in Biochemistry: Applications to Enzyme Systems* (Oxford Univ. Press, New York, 1975).
2. R. B. Moon and J. H. Richards, *J. Biol. Chem.* **248**, 7276 (1973); D. I. Hoult, S. J. W. Busby, D. G. Gadian, G. K. Radda, R. E. Richards, P. J. Seeley, *Nature (London)* **252**, 285 (1974); D. G. Gadian, G. K. Radda, R. E. Richards, P. J. Seeley, in *Biological Applications of Magnetic Resonance*, R. G. Shulman, Ed. (Academic Press, New York, 1979), chap. 10; D. P. Hollis, in *Biological Magnetic Resonance*, L. J. Berliner and J. Reuben, Eds. (Plenum, New York, 1980), vol. 2, chap. 1.
3. W. E. Jacobus, G. J. Taylor, D. P. Hollis, R. L. Nunnally, *Nature (London)* **263**, 756 (1977); P. A. Sehr, G. K. Radda, P. J. Bore, R. A. Sells, *Biochem. Biophys. Res. Commun.* **77**, 195 (1977); A. McLaughlin, H. Takeda, B. Chance, in *Frontiers of Biological Energetics: Electrons to Tissues*, L. Dutton, J. Leigh, A. Scarpa, Eds. (Academic Press, New York, 1978), abstract 172.
4. F. F. Brown, I. D. Campbell, P. W. Kuchel, D. C. Rabenstein, *FEBS Lett.* **82**, 12 (1977); A. Daniels, R. J. P. Williams, P. E. Wright, *Nature (London)* **261**, 321 (1976); D. L. Rabenstein and A. A. Isab, *J. Magn. Reson.* **36**, 281 (1979); R. G. Shulman, T. R. Brown, K. Ugurbil, S. Ogawa, S. M. Cohen, J. A. den Hollander, *Science* **205**, 160 (1979).
5. D. P. Hollis, R. L. Nunnally, W. E. Jacobus, G. J. Taylor, *Biochem. Biophys. Res. Commun.* **75**, 1086 (1977); D. P. Hollis, R. L. Nunnally, G. J. Taylor, M. L. Weisfeldt, W. E. Jacobus, *J. Magn. Reson.* **29**, 319 (1978).
6. J. J. H. Ackerman, T. M. Grove, G. G. Wong, D. G. Gadian, G. K. Radda, *Nature (London)* **283**, 167 (1980).
7. B. N. Singh, G. Ellrodt, C. T. Peter, *Drugs* **15**, 169 (1978); G. Neugebauer, *Cardiovasc. Res.* **12**, 247 (1978); W. G. Nayler and J. Szeto, *ibid.* **6**, 120 (1972); A. Fleckenstein, *Adv. Cardiol.* **12**, 183 (1974).
8. W. G. Nayler, E. Fassold, C. Yepez, *Cardiovasc. Res.* **12**, 152 (1978).
9. S. Mittnacht, S. C. Sherman, J. L. Farber, *J. Biol. Chem.* **254**, 9871 (1979).
10. P. A. Bottomley and R. L. Nunnally, in preparation.
11. B. H. Bulkley, R. L. Nunnally, D. P. Hollis, *Lab. Invest.* **39**, 133 (1978).
12. D. P. Hollis, R. L. Nunnally, G. J. Taylor, M. L. Weisfeldt, W. E. Jacobus, in *Biomolecular Structure and Function*, P. F. Agris, R. N. Laeppkey, B. D. Sykes, Eds. (Academic Press, New York, 1978), p. 217.
13. T. C. Farrar and E. D. Becker, *Pulse and Fourier Transform NMR* (Academic Press, New York, 1971), pp. 37-40.
14. R. L. Nunnally and D. P. Hollis, *Biochemistry* **18**, 3642 (1979); R. L. Nunnally, in *Cardiac Energy Transport*, W. E. Jacobus and J. S. Ingwall, Eds. (Williams & Wilkins, Baltimore, in press).
15. T. H. Grove, J. J. H. Ackerman, G. K. Radda, P. J. Boor, *Proc. Natl. Acad. Sci. U.S.A.* **77**, 299 (1980).
16. This work was supported by NIH grants GM 17172, HL22080, and HL17655-06 and by the S. B. Clayton Fund. We thank B. H. Bulkley for providing the verapamil and for reviewing the manuscript. These experiments were performed while the authors were members of the Departments of Radiology and Physiological Chemistry, Johns Hopkins University School of Medicine, Baltimore, Md.

2 June 1980; revised 6 October 1980

Mutagenicity of Fly Ash Particles in *Paramecium*

Abstract. Paramecium, *a protozoan that ingests nonnutritive particulate matter, was used to determine the mutagenicity of fly ash. Heat treatment inactivated mutagens that require metabolic conversion to their active form but did not destroy all mutagenicity. Extraction of particles with hydrochloric acid, but not dimethyl sulfoxide, removed detectable mutagenic activity.*

The combustion of coal to generate electric power produces vast quantities of fly ash. Although fly ash is considered to be the most abundant industrial solid-waste product in the United States, only a few studies have been performed to evaluate the potential health effects of exposure to fly ash or its leachates. The finest fly ash fractions collected from a power plant smokestack (*1*) were found to be mutagenic in the Ames bacterial assay (*2*, *3*). Since there is a high positive correlation between carcinogenicity of substances for animals and man and mutagenic activity in the Ames test (*4*), the mutagenicity of fine fly ash particles raises concern (*2*, *3*).

A possible mode for an abatement technology was suggested by the finding that heat-treated fly ash loses detectable mutagenic activity due to the decomposition of surface mutagens (*3*, *5*). While agents identified as mutagenic by the Ames test may be presumed to be poten-

Table 1. Mutagenic effect of fly ash and heat-treated fly ash in *Paramecium*. Values not connected by the same line are significantly different from each other (Wilcoxon matched-pairs signed-ranks test, $\alpha = .05$). The data from six experiments were pooled since the control values for autogamous progeny were not significantly different. Cerophyl is the ryegrass extract used for cultivation of *Paramecium*. Induced S-9 is the Ames liver microsome fraction from rats receiving Arochlor 1254 (polychlorinated biphenyl) to activate the enzymes for conversion of promutagens to mutagenic form; uninduced S-9 is from rats receiving corn oil only (the vehicle for the Arochlor). Glass beads (1 to 3 μm) suspended in either induced or uninduced S-9 were used as a negative control for nonnutritive particles. Kaolinite was also used in one experiment, and the results were the same as those for the glass beads. Benzo[*a*]pyrene was the positive control for mutagenicity requiring induced S-9. The initial concentration of suspended fly ash was 535 μg/ml. The average number of affected progeny from treated parent cells was 20 percent higher than the average number of affected control progeny. Since one mutation would theoretically yield only 4 affected progeny in 16 autogamous progeny from a treated parent cell (*6*), the percentages, though low, reflect significant damage.

Substance	Lethal and detrimental cells (%)	Number of progeny examined
Cerophyl	1.01 ± 0.21	1568
Glass beads + uninduced S-9	1.36 ± 0.33	1904
Glass beads + induced S-9	1.41 ± 0.42	1888
Benzo[*a*]pyrene + uninduced S-9	3.2 ± 0.39	1440
Fly ash + uninduced S-9	3.7 ± 0.69	2992
Heated fly ash + uninduced S-9	3.9 ± 1.6	1728
Heated fly ash + uninduced S-9	4.6 ± 1.3	1280
Fly ash + uninduced S-9	9.3 ± 1.7	1296
Benzo[*a*]pyrene + uninduced S-9	12.5 ± 5.8	1664

0036-8075/81/0109-0180$00.50/0